The mapping of the conditional pair density onto the electron density

R. F. W. Bader and G. L. Heard

Citation: The Journal of Chemical Physics **111**, 8789 (1999); doi: 10.1063/1.480226
View online: http://dx.doi.org/10.1063/1.480226
View Table of Contents: http://scitation.aip.org/content/aip/journal/jcp/111/19?ver=pdfcov
Published by the AIP Publishing

The mapping of the conditional pair density onto the electron density

R. F. W. Bader and G. L. Heard
Department of Chemistry, McMaster University, Hamilton Ontario, L8S 4M1 Canada

(Received 30 April 1999; accepted 25 August 1999)

This paper shows that the Fermi hole of a reference electron can be so strongly localized to a given region of space, as to cause the conditional pair density for same-spin electrons to approach the one-electron spin density outside the region of localization and for a closed-shell system, the conditional pair density for both spins will approach the total density. Correspondingly, the Laplacian of the conditional pair density, whose local concentrations indicate the positions where the density of the remaining electrons are most likely to be found for a fixed position of a reference pair, approaches the Laplacian of the density. The Laplacian of the conditional pair density generated by a sampling of pair space by an α,β pair of reference electrons, exhibits a homeomorphism with the Laplacian of the electron density. This homeomorphism approaches an isomorphic mapping of one field onto the other, as the reference electron pair becomes increasingly localized to a given region of space. Thus the local charge concentrations (CCs) displayed by the Laplacian of the electron density, the local maxima in $L(\mathbf{r})=-\nabla^2\rho(\mathbf{r})$, signify the presence of regions of partial pair condensation, regions with greater than average probabilities of occupation by a single pair of electrons, as has been previously surmized on empirical grounds. This paper establishes a mapping of the essential aspects of electron pairing, determined in six-dimensional space, onto the three-dimensional space of the electron density. The properties of the conditional pair density enable one to determine which CCs of $L(\mathbf{r})$ are coupled and represent the same localized pair of electrons. It is found that the pattern and properties of the electron localization domains predicted by the Laplacian of the conditional pair density differ in important aspects from those predicted by ELF, the electron localization function. © *1999 American Institute of Physics.* [S0021-9606(99)30743-1]

PHYSICAL REQUIREMENT FOR THE SPATIAL PAIRING OF ELECTRONS

The formation of localized α,β pairs is a consequence of the pair density being antisymmetric with respect to the exchange of the space and spin coordinates of every pair of electrons, as required by the Pauli exclusion principle. The exclusion is a result of the Fermi hole that is created in the pair density by the antisymmetrization requirement.[1] The Fermi hole has a simple physical interpretation: it may be viewed as a description of how the density of an electron of given spin, the so-called reference electron, is spread out in space, thereby excluding the presence of an identical amount of same-spin density.[2,3] All physical measures of the localization or delocalization of an electron are determined by the corresponding localization or delocalization of its Fermi hole.[4] Since this behavior is obtained separately for an α and a β electron in a closed-shell system, the density of the Fermi hole determines the spatial pairing of the electrons.

In what follows we shall restrict the discussion to the Hartree–Fock level of theory where the only correlation is the Fermi correlation. The addition of Coulomb correlation, while altering the numerical results, does not alter any of the physical interpretations or the understanding of electron localization.[5] At the Hartree–Fock level, there is no correlation between electrons of different spin and the pair density is simply the product of the α and β spin densities multiplied by a factor of one-half (so as not to count the same pair twice), or

$$\rho^{\alpha\beta}(\mathbf{r}_1,\mathbf{r}_2)=(1/2)\rho^{\alpha}(\mathbf{r}_1)\rho^{\beta}(\mathbf{r}_2). \tag{1}$$

For same-spin electrons however, the density at $\mathbf{r}_2$, $\rho^{\alpha}(\mathbf{r}_2)$, is reduced in value by the density of the Fermi hole $h^{\alpha\alpha}(\mathbf{r}_1,\mathbf{r}_2)$, a negative quantity, and the number of same spin pairs is correspondingly reduced, Eq. (2),

$$\rho^{\alpha\alpha}(\mathbf{r}_1,\mathbf{r}_2)=(1/2)\rho^{\alpha}(\mathbf{r}_1)[\rho^{\alpha}(\mathbf{r}_2)+h^{\alpha\alpha}(\mathbf{r}_1,\mathbf{r}_2)]. \tag{2}$$

The density of the Fermi hole, the negative of Slater's exchange charge density,[6] is given by

$$h^{\alpha\alpha}(\mathbf{r}_1,\mathbf{r}_2)=-\sum_{i}^{\alpha}\sum_{j}^{\alpha}[\phi_i^*(\mathbf{r}_1)\phi_i(\mathbf{r}_2)\phi_j^*(\mathbf{r}_2)\phi_j(\mathbf{r}_1)]/\rho^{\alpha}(\mathbf{r}_1). \tag{3}$$

It is a function of the position of the coordinate $\mathbf{r}_1$ assigned to the reference electron labeled e^*. However, e^* is not localized to $\mathbf{r}_1$. Instead the Fermi hole describes how the density of e^* is spread out from this point into the space of another same-spin electron described by the coordinate $\mathbf{r}_2$ and excluding an equivalent amount of density at each $\mathbf{r}_2$. This exclusion effect is described by a conditional density. Division of $\rho^{\alpha\alpha}(\mathbf{r}_1,\mathbf{r}_2)$ in Eq. (2) by $\rho^{\alpha}(\mathbf{r}_1)/2$ yields the *conditional same-spin pair density* $\delta^{\alpha\alpha}(\mathbf{r}_1,\mathbf{r}_2)$, the density of same-spin electrons found at the position $\mathbf{r}_2$ subject to the condition that the reference electron is assigned the coordinate $\mathbf{r}_1$,

$$\delta^{\alpha\alpha}(\mathbf{r}_1,\mathbf{r}_2)=\rho^{\alpha}(\mathbf{r}_2)-|h^{\alpha\alpha}(\mathbf{r}_1,\mathbf{r}_2)| \tag{4}$$

Writing the expression in terms of the absolute value of the Fermi density emphasizes that its role is to reduce the spin density at each position $\mathbf{r}_2$. The conditional pair density is thus a measure of the amount of same-spin density not excluded from the position $\mathbf{r}_2$ by the spreading out of the density of e^* at $\mathbf{r}_1$. The integral of $\delta^{\alpha\alpha}(\mathbf{r}_1,\mathbf{r}_2)$ over the space of the second electron yields $N^\alpha-1$, and hence $\delta^{\alpha\alpha}(\mathbf{r}_1,\mathbf{r}_2)$ describes the spatial disposition of the remaining same-spin electrons for a given position of the reference electron. The value of the Fermi hole is equal to the negative of the same-spin pair density when $\mathbf{r}_2=\mathbf{r}_1$, thereby totally excluding all other same-spin electrons from the reference point, and $\delta^{\alpha\alpha}(\mathbf{r}_1,\mathbf{r}_1)=0$. If this total exclusion of same-spin density persists as $\mathbf{r}_2$ is displaced from $\mathbf{r}_1$, then the hole will describe a region of space from which all other same-spin electrons are excluded. In this situation, the Fermi hole is maximally localized and its density excludes the density of all other same-spin electrons, up to the amount of one electronic charge, from the vicinity of e^* and the density of another same-spin electron is found only outside of this hole. In a closed-shell molecule, the same behavior will be obtained for an electron of opposite spin and the result will be a region of space occupied by the density of a single α,β pair of electrons. If this total degree of exclusion is maintained for motion of the pair of reference electrons over the region of exclusion, the result is a spatially localized electron pair. These properties of $\delta^{\alpha\alpha}(\mathbf{r}_1,\mathbf{r}_2)$ have been previously discussed and illustrated.[4,7] In summary, the requirement for the localization of an electron of either spin to a given region of space, and hence for the formation of a localized pair, is that the density of their Fermi holes be completely contained within the region, thereby excluding all other electrons of either spin.[2]

While this degree of localization of the Fermi hole density, hereafter referred to as the Fermi density, can be approached, it can never be realized. It is most closely approached for core electrons and for atoms in simple ionic systems. It was demonstrated that in these favorable cases, a region could be defined whose contained Fermi correlation was maximized with respect to a variation in its bounding surface and when this occurred the region had a population of 2.00 e and a pair population close to unity.[2] It was also shown that this degree of localization resulted in a region whose population exhibited a minimum in its fluctuation.[8]

THE LAPLACIAN AS A MEASURE OF PARTIAL PAIR CONDENSATION

The Laplacian of the electron density determines where the density $\rho(\mathbf{r})$ is locally concentrated, $\nabla^2\rho(\mathbf{r})<0$, and locally depleted $\nabla^2\rho(\mathbf{r})>0$. For a free atom it exhibits shells of alternating charge concentration and charge depletion that mimic the atomic shell structure, each shell being represented by a pair of regions. The outer shell of charge concentration is referred to as the valence shell of charge concentration (VSCC). The shell structure persists for an atom in a molecule, but the spherical surface over which the density is maximally concentrated in the VSCC of a free atom is distorted by the formation of local maxima (termed local charge concentrations or CCs), minima and saddles on its surface in response to the bonded interactions.[9] It is the topology exhibited by the CCs formed in the surface of charge concentration in the VSCC of a central atom that faithfully maps onto the number, relative size and angular orientation of the bonded and nonbonded electron pair domains whose presence is assumed in the VSEPR model of molecular geometry.[10] The geometrical patterns associated with differing numbers of electron pairs proposed in the VSEPR model were based on the findings obtained by Lennard-Jones in his analysis of the properties of the same-spin pair density[11] and, as a consequence one assumes the existence of a relation between $L(\mathbf{r})$ and the pair density.

The Laplacian of the electron density appears throughout the theory of atoms in molecules[3] and it is used, along with the value of the density at a bond critical point, in a classification of bonding.[12] Since $L(\mathbf{r})$ is related to the experimentally measurable electron density, it is being increasingly determined in such experiments.[13] The observed mapping of the CCs in $L(\mathbf{r})$ with the assumed electron domains of VSEPR is found to be a general result for valence regions whose contained Fermi correlation, while falling short of that required for the localization of a single pair of electrons,[2] is sufficient to result in a significant decrease, relative to a random distribution, in the contributing number of pairs. Studies of the localization of the Fermi density for given positions of the reference electron led to the working assumption that the pattern of local charge concentrations (CCs) defined by the maxima in $L(\mathbf{r})$ denotes a corresponding pattern of *partial condensation* of the pair density that denotes regions of space exhibiting a marked diminution in the number of contributing electron pairs, the limiting situation being the association of one electron pair with each CC.[14]

The concept of partial pair condensation is illustrated by the contrasting behavior of a core and a valence region. The average electron population of the Li atom in LiF is 2.0e and the pair density yields an average pair population of 1.1, values close to the idealized limit of an average population of 2.0e arising from the presence of just a single pair of electrons. However, the electron density in a valence region is, in general, the result of contributions from many electron pairs. The region associated with a nonbonded pair on N in NH_3 for example, while also having an average population of 2.0e, has an average pair population of 2.9.[2] There are ten electrons in ammonia which from 45 distinct pairs of electrons, or 28 excluding the core on N, so that a region with an average pair population of 3 is well below that obtained from a distribution with a random pairing of electrons throughout the molecule. So while the nonbonded region on N in ammonia does not meet the requirements for a single spatially localized electron pair, it does represent a region where the pairing is greatly reduced from the random level, an example of partial pair condensation. Correspondingly, the Laplacian distribution for ammonia exhibits a pronounced maximum in $L(\mathbf{r})$ in the region of the nonbonding density.[3]

RELATING THE TOPOLOGIES OF $\delta^{\alpha\alpha}(\mathbf{r}_1,\mathbf{r}_2)$ AND $L(\mathbf{r})$

Laplacian of the conditional pair density

In a closed-shell molecule, the alpha and beta conditional spin densities are identical. Their sum, Eq. (5), will be denoted by $\delta^{\sigma}(\mathbf{r}_1,\mathbf{r}_2)$ and termed the conditional pair density

$$\delta^{\sigma}(\mathbf{r}_1,\mathbf{r}_2)=\delta^{\alpha\alpha}(\mathbf{r}_1,\mathbf{r}_2)+\delta^{\beta\beta}(\mathbf{r}_1,\mathbf{r}_2). \tag{5}$$

The ''σ'' denotes the inclusion of only same-spin pairs with no contributions from α,β or β,α components to the pair density. The conditional pair density $\delta^{\sigma}(\mathbf{r}_1,\mathbf{r}_2)$ exhibits a local minimum at the position $\mathbf{r}_1$, but like the total density that it can approach in value, it does not exhibit local maxima other than at the positions of nuclei and one must appeal to its Laplacian distribution to reveal its fine structure. An earlier study had shown that if the core orbitals with their dominating spin density are omitted, the topology of $\delta^{\alpha\alpha}(\mathbf{r}_1,\mathbf{r}_2)$ exhibits distinct maxima in regions removed from the position of e^*. The maxima are most pronounced when e^* is placed at a position where $L(\mathbf{r})$ exhibits a maximum, that is, in a region where one has reason to believe the Fermi hole is relatively localized. The investigation demonstrated that the topology of the conditional same-spin pair density defined in this manner is so successful in recovering the geometrical models associated with differing numbers of electron pairs, that it was proposed that the conditional same-spin density be called the Lennard-Jones function or LJF.[7] The work on LJF made it clear that the Fermi density of the reference electron can indeed be sufficiently localized about the point $\mathbf{r}_1$ as to cause its contribution to the conditional pair density at points well removed from the position of the reference electron to become vanishingly small. Under these conditions, Eq. (4) shows that the value of $\delta^{\alpha,\alpha}(\mathbf{r}_1,\mathbf{r}_2)$ at $\mathbf{r}_2$ should approach the spin density $\rho^{\alpha}(\mathbf{r}_2)$. Under the same condition of localization of the reference electron, the value of $\delta^{\sigma}(\mathbf{r}_1,\mathbf{r}_2)$ should approach the total density $\rho(\mathbf{r}_2)$ and its Laplacian should reduce to the Laplacian of the density.

Programs have been written to determine the Laplacian of $\delta^{\sigma}(\mathbf{r}_1,\mathbf{r}_2)$ as a function of $\mathbf{r}_2$, for a fixed value of $\mathbf{r}_1$, the function $\nabla^2(\mathbf{r}_2)\{\delta^{\sigma}(\mathbf{r}_1,\mathbf{r}_2)\}$. The negative of this function is denoted by $L(e^*,\mathbf{r}_2)$, e^* being the position assigned to the reference electron. The program locates and classifies the critical points (CPs) in $L(e^*,\mathbf{r}_2)$ using the full wave function, enabling one to make a detailed comparison of its structure with that exhibited by $L(\mathbf{r})$, as a function of the position assigned to e^*. One is interested in particular in locating the local maxima in $L(e^*,\mathbf{r}_2)$, as these will determine where the conditional density is locally concentrated, that is, where the density arising from other α,β pairs, as separately determined by the two same-spin conditional densities, are most likely to be found for a given positioning of the reference pair.

Pair condensation to yield atomic shell structure

It was noted early on[15] that $L(\mathbf{r})$ exhibits shell structure by displaying alternating pairs of shells of charge concentration (the first one being a spikelike region centred on the nucleus) and charge depletion. It is found that for atoms up to Xe, with the exception of transition metal atoms, the structure determined in this manner duplicates that anticipated on the basis of equating the number of shells to the principal quantum number n.[16,17] For the transition metal atoms $n-1$ such alternating pairs of shells are found. We first demonstrate that $L(e^*,\mathbf{r}_2)$ recovers the shell structure exhibited by $L(\mathbf{r})$ through a comparison of the number of extrema exhibited by $\nabla^2\rho^{\alpha}(\mathbf{r})$ and $\nabla^2(\mathbf{r}_2)\{\delta^{\alpha\alpha}(\mathbf{r}_1,\mathbf{r}_2)\}$ for some ground state atoms with 3 to 5 shells, Fig. 1. The results for the Cr and Mo atoms in their septet spin states refer to the component with maximum M_s value, while those for the closed-shell atoms are one-half the values obtained for the total density. The innermost structure in $\nabla^2(\mathbf{r}_2)\times\{\delta^{\alpha\alpha}(\mathbf{r}_1,\mathbf{r}_2)\}$ was determined by placing e^* at a radius corresponding to the maximum in the VSCC, while the remaining structure is obtained by placing e^* at the nucleus, a position that results in the loss of the inner core structure. The innermost minimum for the shell with $n=1$ occurs at the position of the nucleus.

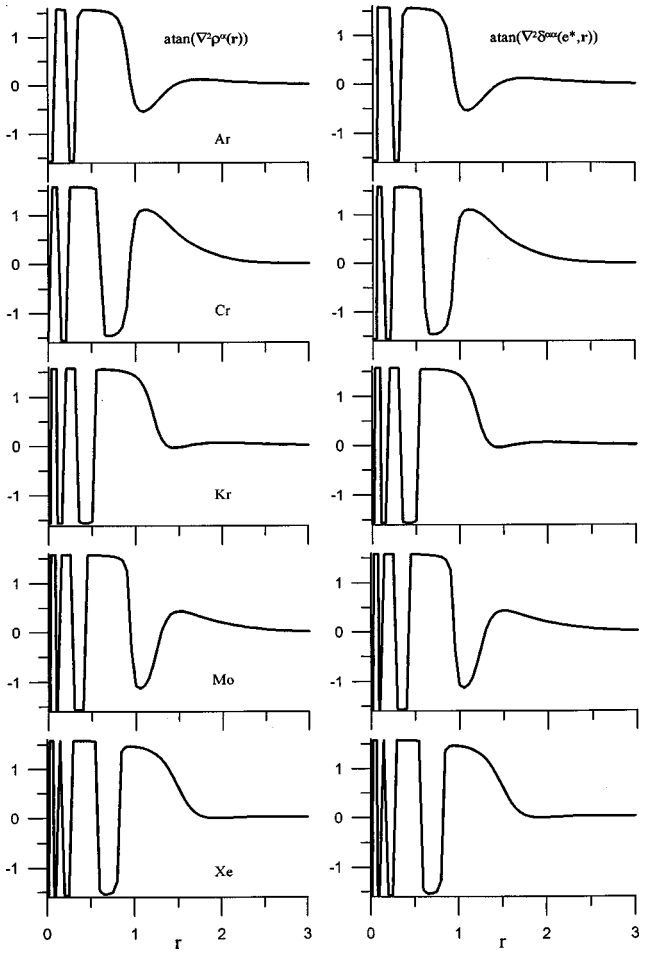

FIG. 1. Comparison of shell structure predicted by the Laplacians of the density and of the same-spin conditional pair density. The value of the atan of each function is plotted in radians versus the coordinate r denoting the distance from the nucleus. The same display is obtained along the vector directed to any point $\mathbf{r}$ in real space (these are not radial distribution functions). The quoted values for $\nabla^2\delta^{\alpha\alpha}(e^*,\mathbf{r})$ are obtained with e^* at the outermost minimum in $L(\mathbf{r})$ for the $n=1$ and 2 shells of Ar, Cr, Mo, and Kr and including $n=3$ for Xe and at the atomic nucleus for the remaining shells. The agreement in the number of shells is apparent. A quantitative comparison is provided by the data in Table I. The value of atan x approaches x for small x.

TABLE I. Atomic shell structure. [a]

Atom and shell		Radius	$-\nabla^2\rho^{\alpha}(\mathbf{r})$	Radius	$-\nabla^2\delta^{\alpha\alpha}(e^*,\mathbf{r})$ [b]
Ar	2	0.238	379.9	0.238	384.5*
	3	1.089	0.6105	1.085	0.6077
Cr	2	0.172	2159	0.173	2036*
	3	0.694	9.550	0.690	9.637
Kr	2	0.108	20 970	0.108	21060*
	3	0.398	191.6	0.396	196.8
	4	1.442	0.036 27	1.443	0.035 44
Mo	2	0.099	57780	0.098	57390*
	3	0.327	802.1	0.326	812.2
	4	1.043	2.167	1.043	2.164
Xe	2	0.084	130 800	0.084	130 200*
	3	0.222	5261	0.223	5043*
	4	0.661	36.36	0.661	36.31
	5	1.938	−0.0006	1.938	−0.0006

[a]Wave functions for Ar and Kr from 6-311+G(2*d*), A. D. McLean and G. S. Chandler, J. Chem. Phys. **72**, 5639 (1980). R. Krishnan, J. S. Binkley, R. Seeger, and J. A. Pople, J. Chem. Phys. **72**, 650 (1980); for Cr (TZV) from A. J. H. Wachters, J. Chem. Phys. **52**, 1033 (1978); for Mo TZV from Y. Sakai, H. Tatewaki, and S. Huzinaga, J. Comp. Chem. **3**, 6 (1980); for Xe, 3-21*G**, K. D. Dobbs and W. J. Hehre, J. Comp. Chem. **7**, 359 (1986).

[b]Starred values are for e^* at the radius of outermost minimum in $\nabla^2\rho(\mathbf{r})$, the remaining values are for e^* at the nucleus.

Table I compares the values of the two Laplacians at the radii at which they attain their minimum values. These are the radii of the shells of maximum concentration in the functions $L(e^*,\mathbf{r}_2)$ and $L(\mathbf{r})$. The radius of a shell for which $\nabla^2(\mathbf{r}_2)\{\delta^{\alpha\alpha}(\mathbf{r}_1,\mathbf{r}_2)\}$ attains a minimum value is the radius at which the extent of condensation of the pair density into contributions from a corresponding number of α,β electron pairs −1, 4, 4, 9, etc., is maximized. Figure 1 and Table I demonstrate complete qualitative agreement between these two functions regarding the number of shells, as well as excellent quantitative agreement in the values of the radii with somewhat lesser agreement in the associated values of the functions. There can be no question but that the shell structure exhibited by $L(\mathbf{r})$ is indeed determined by the same-spin contributions to the pair density.

Both $L(e^*,\mathbf{r}_2)$ and $L(\mathbf{r})$ predict just three shells for Cr in the fourth row of the periodic table and four shells for Mo in the fifth row. Since $L(e^*,\mathbf{r}_2)$ exhibits the same shell structure as does $L(\mathbf{r})$, one is forced to conclude that the outer and penultimate shells of transition metal atoms are not physically distinct in terms of the localization of the density within them. Statements[16] that the number of maxima in $L(\mathbf{r})$ can fail to recover the required number of shells are incorrect, as the ''missing'' shells are not physically present, a result in agreement with the shells predicted by the number of maxima exhibited by the atomic radial distribution functions.[17] Sagar, Ku, and Smith[16] studied the topology of $\nabla^2\rho(\mathbf{r})$ for atoms up to $Z=88$ and argued that its odd numbered zeros are best suited to determine atomic shell structure, noting that the number of extrema exhibited deviations from the orbital model. It is the outermost maximum in $L(\mathbf{r})$ however, the VSCC, that determines the chemistry of an atom[3] and the finding that the VSCC for heavy metal atoms is contiguous with the outer shell of the core is not a deficiency, but as now demonstrated, a reflection of the properties of the same-spin pair density for heavy metal atoms. Thus the chemistry of these elements differs from that of their main group counterparts, differences previously attributed to the same cause, as evidenced in the statement by Gillespie *et al.*[18] ''the 3*d* electrons cannot be clearly identified as either valence shell electrons or core electrons. This special nature of the 3*d* electrons is responsible for most of the unusual properties of the transition metals.'' Thus unsurprisingly, one finds the distortions induced by bonding in the VSCCs of transition metal atoms differ from those found for their main group counterparts, differences that are shown to arise from corresponding differences in the topologies of $L(e^*,\mathbf{r})$. The topology of the Laplacians of the density and of the conditional pair density further emphasize that the concept of shell structure in atoms is independent of the orbital model, being apparent as well in the existence of the periodic table and in the structure exhibited by the experimentally determined radial distribution function and by the grouping of successive ionization potentials.

Localization of the pair condensation within the VSCC caused by bonding

Bonded interactions result in the formation of local maxima, referred to as charge concentrations (CCs), on the surface of maximum charge concentration in the VSCC of an atom. This added structure is recovered by the Laplacian of the conditional pair density and thus the CCs created within the VSCC of an atom represent a further condensation of the pair density within the outer shell towards the limit of individually spatially localized α, β electron pairs. The most important observation to be demonstrated here is that by placing e^* at a sufficient number of positions, one can establish the existence of a homeomorphism between the fields $L(\mathbf{r})$ and $L(e^*,\mathbf{r}_2)$. It is not necessary to limit e^* to any one position to demonstrate this homeomorphism. While the form of $\delta^{\sigma}(\mathbf{r}_1,\mathbf{r}_2)$ and its Laplacian change as $\mathbf{r}_1$, the posi-

TABLE II. Comparison of critical points (cps) in $L(\mathbf{r})$ and $L(e^*,\mathbf{r}_2)$.[a]

Function	Type of cp	Value of function at $\mathbf{r}_2$	$\rho(\mathbf{r}_2)$	Distance to nucleus A
A. CH_4, $q(H)=-0.044e$				
$L(\mathbf{r})$	*b* CC to H2	1.2576	0.2979	1.00 A=C
$L(\mathrm{CCH1},\mathbf{r}_2)$	bonded to H2	1.4130	0.2994	0.970
$L(\mathrm{bCC\ to\ H1},\mathbf{r}_2)$	bonded to H2	1.4010	0.2994	0.977
$L(\mathbf{r})$	CC at H2	25.9848	0.4333	0.005 A=H2
$L(\mathrm{CC\ at\ H1},\mathbf{r}_2)$	H2 maximum	25.8189	0.4333	0.005
$L(\mathrm{bCC\ to\ H1},\mathbf{r}_2)$	H2 maximum	25.9762	0.4333	0.005
$L(\mathrm{bCC\ to\ H2},\mathbf{r}_2)$	H2 maximum	0.4711	0.4315	0.003
B. NH_3 $q(H)=+0.349e$				
$L(\mathbf{r}_2)$	nb CC	2.6323	0.5562	0.748 A=N
$L(\mathrm{bCC},\mathbf{r}_2)$	nonbonded	2.6052	0.4921	0.798
$L(\mathrm{CCH1},\mathbf{r}_2)$	nonbonded	2.5891	0.5693	0.731
$L(\mathbf{r}_2)$	b CC to H1	2.1944	0.4805	0.831 A=N
$L(\mathrm{nbCC},\mathbf{r}_2)$	bonded to H1	2.1475	0.4921	0.798
$L(\mathrm{bCCH2},\mathbf{r}_2)$	bonded to H1	2.1538	0.4864	0.812
$L(\mathrm{CCH2},\mathbf{r}_2)$	bonded to H1	2.1396	0.4887	0.805
$L(\mathbf{r}_2)$	CC at H2	26.0729	0.4364	0.007 $A=H$
$L(\mathrm{nbCC},\mathbf{r}_2)$	H2 maximum	26.0891	0.4364	0.007
$L(\mathrm{bCCH1},\mathbf{r}_2)$	H2 maximum	26.0546	0.4364	0.007
$L(\mathrm{CCH1},\mathbf{r}_2)$	H2 maximum	25.7700	0.4364	0.007
$L(\mathrm{bCCH2},\mathbf{r}_2)$	H2 maximum	0.7748	0.4329	0.004
C. H_2O $q(H)=+0.627e$				
$L(\mathbf{r}_2)$	nbCC	5.3492	0.9427	0.649 A=O
$L(\mathrm{nbCC},\mathbf{r}_2)$	nonbonded	7.2402	0.9680	0.629
$L(\mathrm{bCC},\mathbf{r}_2)$	nonbonded	6.6374	0.9650	0.636
$L(\mathrm{CCH},\mathbf{r}_2)$	nonbonded	7.0962	0.9728	0.631
$L(\mathbf{r}_2)$	bCC to H2	3.3827	0.7445	0.717 A=O
$L(\mathrm{nbCC},\mathbf{r}_2)$	bonded to H2	5.1276	0.7731	0.687
$L(\mathrm{bH1CC},\mathbf{r}_2)$	bonded to H2	4.4382	0.7619	0.698
$L(\mathrm{CCH1},\mathbf{r}_2)$	bonded to H2	4.7551	0.7670	0.691
$L(\mathbf{r}_2)$	CC at H2	25.6940	0.4296	0.009 A=H
$L(\mathrm{nbCC},\mathbf{r}_2)$	H2 maximum	25.7379	0.4296	0.009
$L(\mathrm{bCCH1},\mathbf{r}_2)$	H2 maximum	25.6600	0.4296	0.009
$L(\mathrm{CCH1},\mathbf{r}_2)$	H2 maximum	25.2505	0.4296	0.009
$L(\mathrm{bCCH2},\mathbf{r}_2)$	H2 maximum	1.1733	0.4251	0.004
D. H_2S $q(H)=-0.142e$				
$L(\mathbf{r})$	nb CC1	0.6022	0.1974	1.297 A=S
$L(\mathrm{nbCC2},\mathbf{r}_2)$	nonbonded	0.6731	0.1982	1.289
$L(\mathrm{bCC},\mathbf{r}_2)$	nonbonded	0.6431	0.1978	1.294
$L(\mathrm{CCH},\mathbf{r}_2)$	nonbonded	0.6472	0.1971	1.294
$L(\mathrm{CCS},\mathbf{r}_2)$	nonbonded	0.6012	0.1977	1.295
$L(\mathrm{CCS},\mathbf{r}_2)$	nonbonded	0.6021	0.1977	1.295
$L(\mathbf{r})$	b CC H1	0.6574	0.2211	1.500 A=S
$L(\mathrm{bCCH2},\mathbf{r}_2)$	bonded to H1	0.7043	0.2211	1.446
$L(\mathrm{nbCC},\mathbf{r}_2)$	bonded to H1	0.7420	0.2212	1.430
$L(\mathrm{CCH2},\mathbf{r}_2)$	bonded to H1	0.7068	0.2209	1.440
$L(\mathbf{r})$	CC at H1	22.5620	0.3788	0.006 A=H
$L(\mathrm{nbCC},\mathbf{r}_2)$	H1 maximum	22.4603	0.3788	0.006
$L(\mathrm{bCC2},\mathbf{r}_2)$	H1 maximum	22.5188	0.3788	0.006
$L(\mathrm{CCH2},\mathbf{r}_2)$	H1 maximum	22.3635	0.3788	0.006
$L(\mathrm{CCS},\mathbf{r}_2)$	H1 maximum	22.5548	0.3788	0.006
$L(\mathrm{bCCH1},\mathbf{r}_2)$	H1 maximum	0.9418	0.3772	0.003
E. PH_3 $q(H)=-0.565e$				
$L(\mathbf{r}_2)$	nb CC	0.3398	0.1319	1.443 A=P
$L(\mathrm{CCH1},\mathbf{r}_2)$	nonbonded	0.3397	0.1314	1.445
$L(\mathrm{CCP},\mathbf{r}_2)$	nonbonded	0.3386	0.1317	1.445
$L(\mathbf{r}_2)$	CC at H1	2.2900	0.3865	0.005 A=H
$L(\mathrm{CCH2},\mathbf{r}_2)$	H1 maximum	2.2733	0.3865	0.005
$L(\mathrm{nbCC},\mathbf{r}_2)$	H1 maximum	2.2580	0.3865	0.005
$L(\mathrm{CCP},\mathbf{r}_2)$	H1 maximum	2.2892	0.3865	0.005
F. ClF_3[b] $q(\mathrm{Cl})=+1.629e, q(F_e)=-0.440e, q(F_e)=-0.595e$				
$L(\mathbf{r})$	nb CC e1	1.7634	0.3645	1.129 A=Cl
L(nbCCe2,**r**2)	nonbonded	1.7615	0.3625	1.127
$L(\mathrm{bCCe},\mathbf{r}_2)$	nonbonded	1.7927	0.3647	1.128
$L(\mathrm{bCCa},\mathbf{r}_2)$	nonbonded	1.7564	0.3619	1.135
$L(\mathrm{CCCl},\mathbf{r}_2)$	nonbonded	1.7632	0.3653	1.127
$L(\mathbf{r})$	b CC e	0.3979	0.2524	1.256 A=Cl
$L(\mathrm{nbCCe},\mathbf{r}_2)$	bonded to e	0.5518	0.2526	1.243
$L(\mathrm{bCCa},\mathbf{r}_2)$	bonded to e	0.4537	0.2524	1.260
$L(\mathrm{CCCl},\mathbf{r}_2)$	bonded to e	0.3978	0.2525	1.255
$L(\mathbf{r})$	b CC a1	0.1016	0.1964	1.268 A=Cl
$L(\mathrm{nbCCe},\mathbf{r}_2)$	bonded to a1	0.2561	0.1971	1.258
$L(\mathrm{bCCe},\mathbf{r}_2)$	bonded to a1	0.1607	0.1961	1.268
$L(\mathrm{bCCa2},\mathbf{r}_2)$	bonded to a1	0.1079	0.1964	1.268
$L(\mathrm{CCCl},\mathbf{r}_2)$	bonded to a1	0.1016	0.1964	1.268

[a]All calculations use a 6-311++G(2*d*,2*p*) basis.
[b]''a'' denotes axial position, ''e'' denotes equatorial position.

tion of e^*, is changed, $\delta^\sigma(\mathbf{r}_1,\mathbf{r}_2)$ leaves its fingerprint in the density for every choice of $\mathbf{r}_1$. That is, whatever form the density assumes when $\delta^\sigma(\mathbf{r}_1,\mathbf{r}_2)\Rightarrow\rho(\mathbf{r}_2,)$ that form remains. The homeomorphism in the structure exhibited by the $L(\mathbf{r})$ and $L(e^*,\mathbf{r}_2)$ for various positions of e^* is demonstrated for molecules exhibiting a range of intramolecular interactions.

The data in Table II provide a comparison of the properties of the local maxima or (3, −3) CPs in the two fields for hydrides AH_n with A=C, N, O, P, and S which cover the range from shared to polar interactions. Also included are data for the molecule ClF_3 whose predicted T-shaped geometry is a classic example of the success of the VSEPR model. The associated pictorial displays, Fig. 2 compare $L(\mathbf{r})$ with $L(e^*,\mathbf{r}_2)$. The homeomorphism between the two fields is immediately apparent, including the shell structure of the A atom. The distances of the maxima from the A nucleus in the two fields differ in general, by less than 0.04 au and the essential features of the angular distribution of the CCs in $L(\mathbf{r})$ are also recovered. In H_2O and H_2S the angle subtended at the A nucleus by the two nonbonded CCs in $L(\mathbf{r})$ exceeds the tetrahedral value, equalling 128° and 121°, respectively, while the corresponding angle formed by the two smaller bonded CCs is less than tetrahedral, equalling 106° and 95°, respectively. The corresponding nonbonded angles in $L(e^*,\mathbf{r}_2)$ with e^* at the position of a bonded CC in $L(\mathbf{r})$ are 121° and 140°, while the bonded angles with e^* at the position of a nonbonded CC in $L(\mathbf{r})$ are 106° and 92.8°. In NH_3, the angle subtended at N by the nonbonded and bonded CCs in $L(\mathbf{r})$ is 138° while the corresponding angle in $L(e^*,\mathbf{r}_2)$ with e^* at the position of nonbonded CC in $L(\mathbf{r})$ is 141°.

The homeomorphism extends to CPs with a signature other than −3. The CCs or (3, −3) CPs of $L(\mathbf{r})$ present in

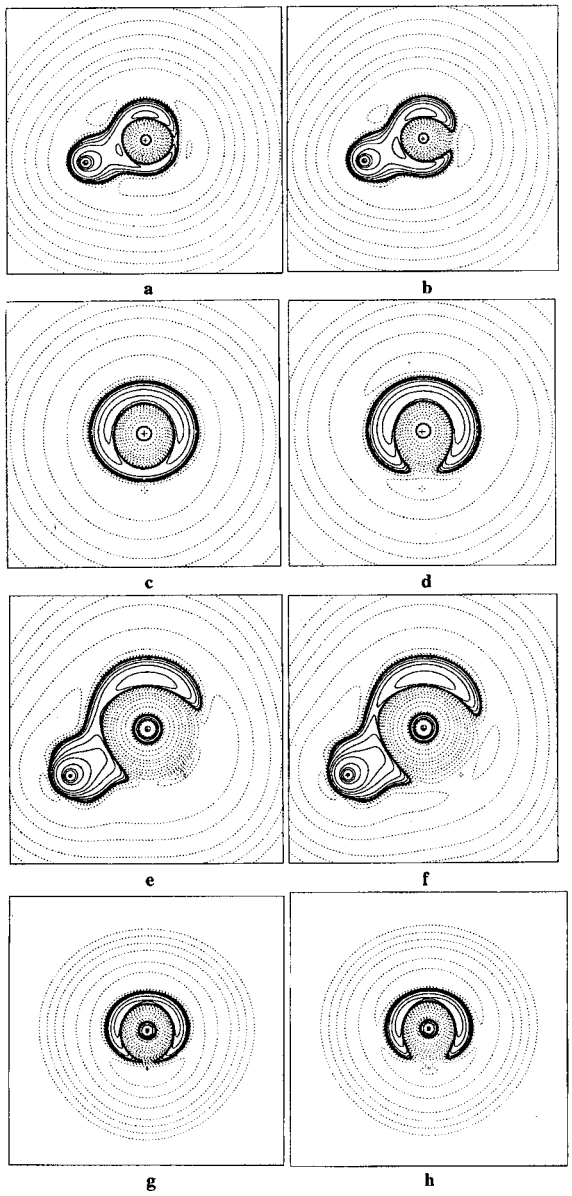

FIG. 2. Comparisons of $L(\mathbf{r})$ and $L(e^*,\mathbf{r})$ in an AH plane for NH_3(**a,b**), and PH_3(**e,f**) and in the nonbonded plane of H_2O(**c,d**) and H_2S(**g,h**). The reference electron is placed at an out-of-plane bonded CC in NH_3, H_2O, and H_2S and at an out-of-plane proton in PH_3. Solid contours denote positive function values, dashed contours, negative values. The homeomorphism between the two fields is evident. Note the presence of two shells for N and O and of three shells for P and S. The values of the functions at their maxima are given in Table II. The values of the contours in au, in this and the following displays are $\pm 2\times 10^n, \pm 4\times 10^n, \pm 8\times 10^n$ with n beginning at -3 and increasing in steps of unity. A zero contour separates the dashed from the solid contours.

the VSCC of an atom define the vertices (V) of a polyhedron, the atomic graph, whose edges (E) are defined by the unique pair of trajectories originating at intervening $(3,-1)$ CPs and with each face (F) containing a $(3,+1)$ CP. The atomic graph is denoted by the characteristic set $[V,E,F]$ giving the number of each type of CP.[3] The atomic graphs for C and N in their hydrides are [4,6,4] and the same set is obtained for $L(e^*,\mathbf{r}_2)$.[4] For example, the CP located at the break in the VSCC of the N atom in Fig. 2 is a F CP with an E CP located between the bonded and nonbonded maxima for both fields. The atomic graph for O in water is [4,5,3] and the CP located along the symmetry axis at the top of the VSCC is an E CP while the one below it on the same axis is a F CP for both fields.

The data in Table II indicate that the homeomorphism approaches an isomorphism in the case of third row elements, particularly when e^* is placed at the nucleus of the heavy atom. (The inner shell structure is recovered by the other placements of e^*). Placing e^* at the position of a second row nucleus does not localize the associated Fermi hole sufficiently to yield a faithful homeomorphism between the two fields. One notes that the homeomorphic mapping does not necessarily deteriorate with a decrease in the distance from the position of e^*. For all the hydrides, the best agreement in the properties of the two fields at the positions of a nonbonded CC, a bonded CC and at a proton are obtained when e^* is placed at a bonded CC rather than at the more removed position on one of the protons. Placing e^* at a bonded CC also yields closer agreement between the two fields than when placed at a nonbonded position.

Placing e^* at the position of a nonbonded CC in H_2O or H_2S does not result in the loss of the second nonbonded maximum in $L(e^*,\mathbf{r})$, Table II, and two separate sets of electron pairs are therefore, necessarily involved. However, absent from Table II are entries corresponding to the bonded maximum associated with the proton bearing e^*. Placement of e^* at a proton results not only in the loss of the protonic maximum but also in the loss of its associated bonded maximum, demonstrating that the Fermi density of a single pair is responsible for both maxima. While placement of e^* at the bonded CC does not result in the complete loss of the large associated maximum at the proton, it is greatly reduced in value. This is a most important observation for it means that the placement of e^* can be used to determine which CCs are coupled and which arise from separate sets of paired electrons. Thus, since the protonic and its associated bonded CC are coupled in the hydrides, the eight CCs in CH_4, the seven in NH_3 and the six in H_2O and H_2S, represent four distinct electron pairs in each molecule. In PH_3 the transfer of electronic charge to the hydrogens, $q(H)=-0.57e$, is sufficient to cause the bonded CCs to merge with the protonic maxima and in this case the four electron pairs generate just four CCs.

The relative magnitudes of the maxima found in ClF_3 for the two fields are in the order nonbonded $>$equatorial bonded$>$axial bonded, as predicted by the VSEPR model. The data for e^* placed at the Cl nucleus illustrate the approach to an isomorphic mapping of the two fields afforded by this example. One notes that all five of the electron domains whose presence determines both the geometry and the chemistry of this molecule, are uncoupled, as placement of e^* at any one of the five CCs in the VSCC of Cl, generates the remaining four, Table II. There are therefore, five contributing electron pairs.

Partial pair condensation in bound transition metal atoms

The VSEPR model can fail to predict the correct geometry when a transition metal or heavy metal atom ($n\geqslant 4$)

serves as the central atom for the assignment of the electron pair domains. Since the topology of $L(\mathbf{r})$ provides a model-free determination of the spatial localization of the electrons that is present in any system, it can be used to determine the characteristics of the pair condensation for a bound transition metal atom and how they might differ from those for a main group atom. This has been done for a wide selection of molecules containing transition and the preceding group II metal atoms.[4,7,19] Firstly, these studies establish that it is indeed the outer shell of the core that is the valence shell, the VSCC, of a transition or heavy metal atom. This result is anticipated from the atomic shell structure displayed by both $L(e^*,\mathbf{r}_2)$ and $L(\mathbf{r})$ and is in accord with the finding that the charge on a bound metal atom is in general, $\geqslant 2$ corresponding to the loss of the two outer *s* electrons. It is also found that, like main group molecules, the VSCC of the bonded metal atom exhibits a characteristic number of CCs and that the geometrical arrangement of these CCs appears to determine the most stable geometry of the molecule using a set of VSEPR-like rules. That is, the most stable geometry is the one that maximizes the separations between the CCs or between the ligands and the CCs.

There is however, one important difference in the behavior of the CCs in the two cases that is most easily visualized in terms of the characteristic polyhedron generated by the CCs within the VSCC of the central atom. In a main group molecule the ligands are adjacent to some or all (depending on the number of nonbonded electron pairs) of the vertices of the polyhedron. In molecules containing a metal atom, the ligands are adjacent to some or all of the faces of the same polyhedron. Thus for a bound main group atom, the ligands are linked to the local concentrations of electronic charge in its VSCC while for a bound metal atom, the ligands are linked to the critical points in the faces of the polyhedron that represent the sites of greatest charge depletion within the VSCC. In effect, a main group atom exhibits *bonded* CCs while a metal atom exhibits *ligand opposed* CCs.

The VH_5 molecule provides an example of the differing behavior between a bound metal and main group atom. The predicted geometry is that of a square based pyramid,[19] as opposed to the trigonal bipyramid geometry anticipated by VSEPR. The CCs in the VSCC of the V atom also form a square based pyramid, but inverted with respect to the arrangement of the ligands such that each ligand is adjacent to one of its faces and the CCs are ligand opposed. Figure 3 compares $L(\mathbf{r})$ and $L(e^*,\mathbf{r}_2)$ for two positions of e^*:e^* at the axial proton illustrates the identical shell structure exhibited by both fields and the ligand opposed nature of the CCs in the VSCC of the vanadium atom, while the map for e^* at an out-of-plane basal proton displays the resulting near isomorphic mapping of the two fields in the indicated plane. The data in Table III compare the properties of the protonic and ligand opposed maxima in $L(e^*,\mathbf{r}_2)$ and $L(\mathbf{r}_2)$ for various positions of e^*. The two fields are again homeomorphic, the mapping approaching an isomorphism by placement of e^* at the V nucleus. Similar agreement is obtained for other transition metal molecules, as was found in the original investigation of the topology of the Lennard-Jones function.[7] There appears to be a weak coupling between the maxima in

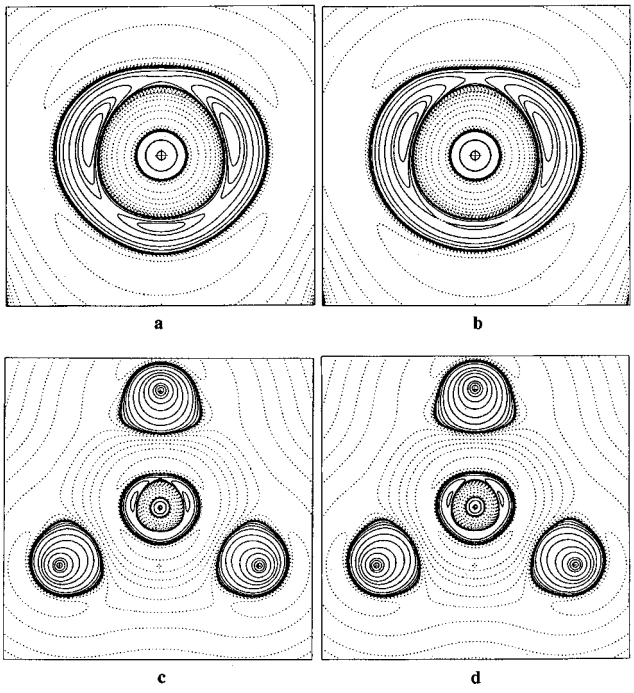

FIG. 3. Comparisons of $L(\mathbf{r})$ (**a** and **c**) and $L(e^*,\mathbf{r})$ (**b** and **d**) for VH_5. Diagrams **a** and **b** are an enlargement of the VSCC of the vanadium atom. All diagrams are for a plane containing the apical proton (H_a) and two basal protons with e^* at H_a in **b**. They illustrate the ligand opposed nature of the maxima in the VSCC of the V atom and the presence of three shells: **a** and **b** contain two extra contours: 13.5 and 16.0 au. The maximum opposed to H_a in **b** is reduced in magnitude from the corresponding CC in **a**. In **d**,e^* is placed at an out-of-plane H_b and the functions in the illustrated plane approach isomorphic behavior.

$L(e^*,\mathbf{r})$ located at a proton and at its associated ligand opposed position. The ligand opposed maxima are present for placements of e^* at both the axial (see Fig. 3) and basal protons but their magnitudes are reduced, more so than for other listed positionings of e^*, Table III. The one opposed to the basal H is also displaced towards the base of the pyramid by $\sim 10°$. The density of the Fermi hole at the position of the proton and its ligand opposed maximum are not completely independent. The ligand opposed nature of the CCs for bound transition metal atoms is also observed in the experimentally determined electron densities of crystals.[20] The pattern of electron localization predicted by the calculated and observed ligand opposed CCs in the VSCC of a transition or heavy metal atom is thus unequivocally related to the properties of the same-spin pair density. The fundamental difference between transition metal and main group atoms in the spatial pairing of their outer electrons provides a rationale for their differing chemistry.

Comparison of topologies of ELF and of Laplacian of conditional pair density

Another frequently used measure of localization is the electron localization function (ELF) of Becke and Edgecombe[21] and it is necessary to compare its predictions with those obtained from the Laplacian of the conditional pair density. The static topology of ELF was first studied by Silvi and Savin[22] and they and their co-workers have used

TABLE III. Comparison of maxima in $L(\mathbf{r})$ and $L(e^*,\mathbf{r})$ for VH_5.[a]

Function	Type of cp	Value of function at $\mathbf{r}_2$	$\rho(\mathbf{r}_2)$	Distance to nucleus A
$L(r)$	CC at H_a	32.4837	0.3709	0.002 A=H_a
$L(CCH_b,r_2)$	maximum at H_a	35.2129	0.4025	0.001
$L(CCoppH_a,r_2)$	maximum at H_a	32.3120	0.4025	0.001
$L(CCoppH_b,r_2)$	maximum at H_a	34.4143	0.4025	0.001
$L(r)$[b]	CC at H_b	35.2441	0.4125	0.001 A=H_b
$L(CCH_a,r_2)$	maximum at H_b	32.4541	0.3709	0.002
$L(CCtransH_b,r_2)$	maximum at H_b	32.0403	0.3709	0.002
$L(CCcisH_b,r_2)$	maximum at H_b	32.0527	0.3709	0.002
$L(CCoppH_b,r_2)$	maximum at H_b	29.2694	0.3709	0.002
$L(CCoppH_bt,r_2)$	maximum at H_b	32.4783	0.3709	0.002
$L(CCoppH_bc,r_2)$	maximum at H_b	31.3365	0.3709	0.002
$L(CCoppH_a,r_2)$	maximum at H_b	32.0220	0.3709	0.002
$L(r)$	CC opp to H_a	17.7988	1.7794	0.718 A=V
$L(CCV,r_2)$	max opp to H_a	17.8897	1.7859	0.716
$L(CCH_a,r_2)$	max opp to H_a	13.7237	1.7513	0.727
$L(CCH_b,r_2)$	max opp to H_a	18.4909	1.7733	0.718
$L(CCppH_b,r_2)$	max opp to H_a	19.2634	1.7833	0.715
$L(r)$	CC opp to H_b	24.0795	2.0371	0.708
$L(CCV,r_2)$	max opp to H_b	24.2255	2.0450	0.706
$L(CCH_a,r_2)$	max opp to H_b	23.9108	2.0273	0.711
$L(CCH_b,r_2)$	max opp to H_b	20.7722	1.9396	0.716
$L(CCtransH_b,r_2)$	max opp to H_b	25.5530	2.0462	0.706
$L(CCcisH_b,r_2)$	max opp to H_b	22.5501	2.0207	0.711
$L(CCoppH_a,r_2)$	max opp to H_b	26.4358	2.0479	0.706
$L(CCoppH_bt,r_2)$	max opp to H_b	23.8474	2.0337	0.709
$L(CCoppH_bc,r_2)$	max opp to H_b	27.4031	2.0542	0.703

[a]H_a denotes axial proton, H_b denotes basal proton.
[b]$CCoppH_bt$ denotes CC opposed to H_b that is trans to H_b; $CCoppH_bc$ denotes same for a cis related H_b.

the dynamics of ELF topology in the study of bond formation.[23,24,25] While a general homeomorphism has been established between the fields $L(\mathbf{r})$ and ELF,[4] a number of important differences are found.

In an expansion of the exchange energy, Becke[26] showed that the leading term in the Taylor series expansion of the spherically averaged same-spin conditional pair probability, Eq. (4), is proportional to a quantity Δ that represents the difference between the positive definite form of the kinetic energy density $G(\mathbf{r})$ and its Weiszäcker form $g(\mathbf{r})$ expressed in terms of the total density $\rho(\mathbf{r})$,

$$\Delta(\mathbf{r})=G(\mathbf{r})-g(\mathbf{r})=(\hbar^2/8m)\sum_i \lambda_i \nabla\rho_i(\mathbf{r})\cdot\nabla\rho_i(\mathbf{r})/\rho_i(\mathbf{r}) - (\hbar^2/8m)\nabla\rho(\mathbf{r})\cdot\nabla\rho(\mathbf{r})/\rho(\mathbf{r}), \quad (6)$$

where λ_i is the occupation number of a set of Hartree–Fock or natural orbitals ϕ_i with corresponding densities $\rho_i=|\phi_i|^2$: $g(\mathbf{r})$ is the correct form of the kinetic energy for system described by a single orbital. The function $\Delta(\mathbf{r})$ was introduced by Tal and Bader in a study of kinetic energy functionals.[27] It was demonstrated that $\Delta(\mathbf{r})\geqslant 0$ and that its vanishing requires that each orbital in a many-electron system be localized to its own region of space. This is the very condition previously shown[2] to be required for the spatial localization of the Fermi hole, leading to the realization that the kinetic energy density contains information regarding the spatial localization of electrons.[27] The reason this should be so is easy to understand: when the orbitals are localized to separate spatial regions, $G(\mathbf{r})$ reduces locally to $g(\mathbf{r})$ and only one electron of each spin contributes to the kinetic energy in each such region. Thus $g(\mathbf{r})$ provides an excellent model of the kinetic energy density in LiH where the molecular orbitals and hence the Fermi density are strongly localized within each atomic basin.[4,27]

Becke and Edgecombe noted that $\Delta(\mathbf{r})$ is itself not suited for measuring the degree of electron localization. Hence they proposed its incorporation into a ''more or less arbitrary'' [21] function ELF denoted by the symbol $\eta(\mathbf{r})$ and defined as

$$\eta(\mathbf{r})=(1+\chi^2)^{-1}, \quad (7)$$

where $\chi=\Delta^\alpha/\Delta_0^\alpha$, and where the quantities are defined for a given spin density. The quantity Δ_0^α is analogous to Δ^α but for a uniform electron gas with same spin density as the system in question. Thus one has $0\leqslant\eta(\mathbf{r})\leqslant 1$ with $\eta(\mathbf{r})=1$ denoting complete localization and $\eta(\mathbf{r})=1/2$ corresponding to uniform electron gaslike behavior.

While $\eta(\mathbf{r})$ is related to the conditional density $\delta^\sigma(\mathbf{r}_1,\mathbf{r}_2)$ through the incorporation of Δ, there is no assurance that the topology of the Laplacian of $\delta^\sigma(\mathbf{r}_1,\mathbf{r}_2)$, which is what determines the spatial localization of the pair density, survives its indirect incorporation into ELF. It is clear for example, that since the atomic shell structure predicted by $L(e^*,\mathbf{r}_2)$ is in agreement with that predicted by $L(\mathbf{r})$, the finding of the missing shells by $\eta(\mathbf{r})$ compared to those predicted by $L(\mathbf{r})$,[21] puts ELF in disagreement with this property of $L(e^*,\mathbf{r}_2)$. The comparison of the topologies of $L(\mathbf{r})$ and $\eta(\mathbf{r})$ previously reported was extensive, with the characteristic set of critical points being given for both fields for a large number of molecules.[4] In general, the two fields are found to be homeomorphic: all of the molecules considered above in Tables II and III for example, give the same characteristic set for both fields. One important difference was noted: in all cases, the radial distance from a nucleus at which the local maximum in $\eta(\mathbf{r})$ is found is always greater, generally by 0.5 to 1.0 au, than in $L(\mathbf{r})$. Since there is close agreement in the radial distances observed for $L(\mathbf{r})$ and $L(e^*,\mathbf{r}_2)$, the distances determined by $\eta(\mathbf{r})$ overestimate the separation of the centers of the domains of electron localization from the associated nucleus. The radii of the shells for which $\eta(\mathbf{r})$ attains its maxima values for the free atoms also exceed the values for corresponding maxima in $L(\mathbf{r})$ and $L(e^*,\mathbf{r})$: the outer radii in Ar, Kr, and Xe for $\eta(\mathbf{r})$ are 1.35, 2.00, and 2.40 au,[20] all greater than the corresponding values in Table I. These results suggest that the element of arbitrariness introduced into the definition of $\eta(\mathbf{r})$ by measuring the smallness of Δ relative to that of a uniform electron gas, while not generally affecting the number or angular distribution of the of the maxima for a bound atom, does artificially increase their radial distances.

The most striking difference in the patterns of electron localization predicted by $L(\mathbf{r})$ and $\eta(\mathbf{r})$ occurs in the description of homonuclear bonding. The carbon-carbon link in both ethane and ethylene is represented in $L(\mathbf{r})$ by a coupled pair of bonded CCs, one within the basin of each carbon atom while in ethyne, a single central bonded maximum is present. In each of these cases a different pattern of localiza-

TABLE IV. Comparison of maxima in $L(\mathbf{r})$ and $L(e^*,\mathbf{r})$ for N_2, and C_2H_4, and C_2H_2.

Function	Type of cp	Value of function at $\mathbf{r}_2$	$\rho(\mathbf{r}_2)$	Distance to nucleus A
N_2 $L(r)$	nbCC on N1	2.9217	0.5779	0.733 A=N1
L(nbCC N1,r_2)	nb max on N2	2.8993	0.5774	0.733 A=N2
L(bCC N1,r_2)	nb max on N1	2.4763	0.5639	0.748 A=N1
L(bCC N1,r_2)	nb max on N2	2.5740	0.5678	0.743 A=N2
N_2 $L(r)$	b CC on N1	3.9633	0.7738	0.824 A=N1
L(nbCC N1,r_2)	b max on N1	2.7618	0.7708	0.859 A=N1
L(nbCC N1,r_2)	b max on N2	2.8412	0.7710	0.857 A=N2
C_2H_4 $L(r)$	b max to H	1.4051	0.3122	0.994 A=Cl
L(CC on H1,r_2) [a]	b max to H2 [a]	1.5206	0.3133	0.969 A=Cl
L(CC on H1,r_2)	b max to H3 H4 [a]	1.3965	0.3122	0.994 A=C2
C_2H_4 $L(r)$	b CC on C1	1.4784	0.3769	0.977 A=Cl
L(CC on H1,r_2)	b max on C1	1.5593	0.3768	0.954 A=Cl
L(CC on H1,r_2)	b max on C2	1.4530	0.3765	0.984 A=C2
C_2H_2 $L(r)$	b CC to H2	1.4798	0.3231	0.970 A=C2
L(CC on H1,r_2)	b max to H2	1.4784	0.3232	0.970 A=C2
L(bCC,r_2)	b max to H2	1.3878	0.3228	0.973 A=C2
C_2H_2 $L(r)$	central b CC	1.5249	0.4388	1.114 A=C1
L(CC on H,r_2)	central max	1.3378	0.4388	1.123 A=Cl

[a]H1 and H2 are bonded to C1, H3 and H4, and C2.

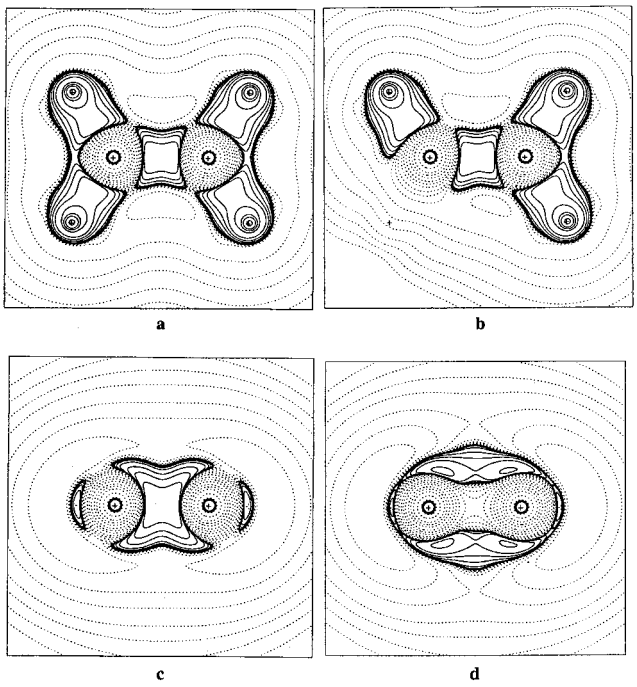

FIG. 4. Comparisons of $L(\mathbf{r})$ and $L(e^*,\mathbf{r})$ for ethene in the plane of the nuclei for **a** and **b** and for the perpendicular plane containing the C–C axis in **c** and **d**. In **b**,e^* is at one of the protons, in **d** it is at the position of a bonded CC on one of the carbons. In **b** the maxima corresponding to the CC at the proton and its adjacent bonded CC are missing for the proton bearing e^* showing that these two CCs in $L(\mathbf{r})$ are coupled. The same behavior is obtained for the maxima corresponding to the two bonded CCs when e^* is placed at the position of one of them. Note the appearance of new maxima in the vicinity of each carbon above and below the molecular plane when e^* is placed at a bonded maximum.

tion is predicted by $\eta(\mathbf{r})$: in ethane a single central maximum is predicted; in ethene two maxima midway between the two carbons are predicted, symmetrically placed on either side of the molecular plane in a manner mimicking the two lobes of a π bond while in ethyne, a central ring attractor is predicted.[4,22] In N_2, $L(\mathbf{r})$ again exhibits a coupled pair of bonded CCs which, in this instance, are replaced by a single central maximum in $\eta(\mathbf{r})$.

Placing e^* at a nonbonded CC in N_2 results in the creation of two bonded maxima and the second nonbonded maximum, with all three CPs exhibiting values and radii similar to the corresponding CPs in $L(\mathbf{r})$, Table IV. The central maximum found in ELF is not present in $L(e^*,\mathbf{r})$. Similar agreement between $L(\mathbf{r})$ and $L(e^*,\mathbf{r})$ is found by placing e^* at a proton in ethane, ethene or ethyne which results in the duplication of all the bonded maxima found in the corresponding $L(\mathbf{r})$ map with the exception of the bonded CC associated with the proton bearing e^*, Table IV. As for the other hydrides, placing e^* at a proton results in a concomitant loss of its associated bonded maximum, indicating the involvement of a single electron pair, an effect made evident in Figs. 4(a) and 4(b). The localizations predicted by ELF for the C–C bonding in C_2H_4 and C_2H_2 are not observed in $L(e^*,\mathbf{r})$.

A coupling is also found between the pair of bonded CCs associated with C–C bonding in ethane, and ethene and with N–N bonding in N_2: placing e^* at one of the bonded CCs in any of these molecules results in the loss of both axial maxima in displays of $L(e^*,\mathbf{r})$. These results indicate that the pair of bonded CCs exhibited in $L(\mathbf{r})$ for a single or a multiple bond are generated by a coupled set of one or more electron pairs. A new feature appears in the properties of $L(e^*,\mathbf{r})$ for placement of e^* at a bonded CC in ethene or ethyne: in ethene the two axial CCs are replaced with four new maxima in the plane perpendicular to the plane of the nuclei, symmetrically placed with respect to the C nuclei, Fig. 4(d), while in ethyne, the single bonded axial maximum is replaced by two tori, each associated with the basin of a single carbon. The π-like maxima formed in ethene are of much smaller (16%) magnitude than the ones they replace, the same being true of the tori formed in ethyne. Thus placing e^* at a CC associated with multiple bonding in ethene and ethyne has the appearance of removing the sigma contribution to the bonding, leaving the contributions from the π density in coupled pairs on both atoms.

CONCLUSIONS

We have found that the Laplacian of the conditional pair density for same-spin electrons, $L(e^*,\mathbf{r})$, can be homeomorphically mapped onto the the Laplacian of the electron density $L(\mathbf{r})$ by placement of the reference electron e^* at positions of maximum localization of the Fermi hole for an α,β electron pair. The mapping appears faithful in that every maximum in $L(\mathbf{r})$ can be associated with a corresponding maximum in $L(e^*,\mathbf{r})$. The mapping indicates that the CCs of $L(\mathbf{r})$ denote the spatial regions in which there is a partial condensation of the pair density towards individually localized electron pairs. Unlike $L(\mathbf{r})$, which is the limiting form assumed by $L(e^*,\mathbf{r})$ for complete localization of the Fermi hole of e^*, ELF has no direct relationship to $L(e^*,\mathbf{r})$. Work is in progress to determine the Laplacian of the difference function $\Delta(\mathbf{r})$, Eq. (6), the component in ELF[21] that mea-

sures the degree of pair condensation,[27] to determine if this function, without further manipulation, yields regions of concentration that map onto those displayed by $L(e^*,\mathbf{r})$.

ACKNOWLEDGMENT

We thank Dr. P. J. MacDougall for providing helpful comments.

[1] R. McWeeny, Rev. Mod. Phys. **32**, 335 (1960).
[2] R. F. W. Bader and M. E. Stephens, J. Am. Chem. Soc. **97**, 7391 (1975).
[3] R. F. W. Bader, *Atoms in Molecules-A Quantum Theory* (Oxford University Press, Oxford UK, 1990).
[4] R. F. W. Bader, S. Johnson, T.-H. Tang, and P. L. A. Popelier, J. Phys. Chem. **100**, 15398 (1996).
[5] X. Fradera, M. A. Austen, and R. F. W. Bader, J. Phys. Chem. A **103**, 304 (1999).
[6] J. C. Slater, Phys. Rev. **81**, 385 (1951).
[7] R. J. Gillespie, D. Bayles, J. Platts, G. L. Heard, and R. F. W. Bader, J. Phys. Chem. A **102**, 3407 (1998).
[8] R. F. W. Bader and M. E. Stephens, Chem. Phys. Lett. **26**, 445 (1974).
[9] R. F. W. Bader, P. J. MacDougall, and C. D. H. Lau, J. Am. Chem. Soc. **106**, 1594 (1984).
[10] R. J. Gillespie and I. Hargittai, *The VESPR Model of Molecular Geometry* (Allyn and Bacon and Prentice Hall International, Boston, MA, 1991).
[11] J. E. Lennard-Jones, Proc. Soc. London, Ser. A **198**, 14 (1949).
[12] R. F. W. Bader and H. Essén, J. Chem. Phys. **80**, 1943 (1984).
[13] M. A. Spackman, Ann. Rep. Roy. Soc. Chem. Section C **94**, 177 (1998).
[14] R. F. W. Bader, R. J. Gillespie, and P. J. MacDougall, J. Am. Chem. Soc. **110**, 7329 (1988).
[15] R. F. W. Bader and P. M. Beddall, J. Chem. Phys. **56**, 3320 (1972).
[16] R. P. Sagar, A. C. T. Ku, and V. H. Smith, J. Chem. Phys. **88**, 4367 (1988).
[17] Z. Shi and R. J. Boyd, J. Chem. Phys. **88**, 4375 (1988).
[18] R. J. Gillespie, D. A. Humphreys, N. C. Baird, and E. A. Robinson, *Chemistry* (Allyn and Bacon, Boston, 1986), p. 763.
[19] I. Bytheway, R. J. Gillespie, T.-H. Tang, and R. F. W. Bader, Inorg. Chem. **34**, 2407 (1995); R. J. Gillespie, I. Bytheway, T.-H. Tang, and R. F. W. Bader, *ibid.* **35**, 3954 (1996).
[20] G. T. Smith, P. R. Mallinson, C. S. Frampton, L. J. Farrugia, R. D. Peacock, and J. A. K. Howard, J. Am. Chem. Soc. **119**, 5028 (1997); C. C. Wang, H.-J. Liu, K.-J. Lin, L.-K. Chou, and K.-S. Chan, J. Phys. Chem. A **101**, 8887 (1997); T. S. Hwang and Y. Wang, J. Phys. Chem. A **102**, 3726 (1998); C.-R. Lee, C.-C. Wang, K.-C. Chen, G.-H. Lee, and Y. Wang, J. Phys. Chem. A **103**, 156 (1999).
[21] A. D. Becke and K. E. Edgecombe, J. Chem. Phys. **92**, 5397 (1990).
[22] B. Silvi and A. Savin, Nature (London) **371**, 683 (1994).
[23] X. Krokidis, S. Noury, and B. Silvi, J. Phys. C **101**, 7277 (1997).
[24] S. Noury, F. Colonna, A. Savin, and B. Silvi, J. Mol. Struct. **450**, 59 (1998).
[25] A. Beltran, J. Andres, S. Noury, and B. Silvi, J. Phys. Chem. A (in press).
[26] A. D. Becke, Int. J. Quantum Chem. **23**, 1915 (1983).
[27] Y. Tal and R. F. W. Bader, Int. J. Quantum Chem., Symp. **12**, 153 (1978).